PAPER

Incorporation of detailed eye model into polygon-mesh versions of ICRP-110 reference phantoms

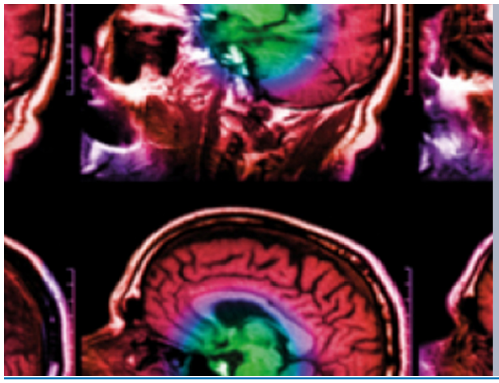

IOP Publishing | Institute of Physics and Engineering in Medicine Physics in Medicine & Biology

Phys. Med. Biol. **60** (2015) 8695–8707 doi:10.1088/0031-9155/60/22/8695

Incorporation of detailed eye model into polygon-mesh versions of ICRP-110 reference phantoms

Thang Tat Nguyen[1], Yeon Soo Yeom[1], Han Sung Kim[1], Zhao Jun Wang[1], Min Cheol Han[1], Chan Hyeong Kim[1], Jai Ki Lee[1], Maria Zankl[2], Nina Petoussi-Henss[2], Wesley E Bolch[3], Choonsik Lee[4] and Beom Sun Chung[5]

[1] Department of Nuclear Engineering, Hanyang University, 222 Wangsimni-ro, Seongdong-gu, Seoul 133-791, Korea
[2] Research Unit Medical Radiation Physics and Diagnostics, Helmholtz Zentrum München Deutsches Forschungszentrum für Gesundheit und Umwelt (GmbH), Ingolstädter Landstraße 1, D-85764 Neuherberg, Germany
[3] J Crayton Pruitt Family Department of Biomedical Engineering, University of Florida, PO Box 116131, Gainesville, FL 32611-6131, USA
[4] Division of Cancer Epidemiology & Genetics, National Cancer Institute, 9609 Medical Center Drive, Bethesda, MD 20892-9760, USA
[5] Department of Anatomy, Ajou University School of Medicine, 443-380, 164 Worldcup-ro, Suwon, Korea

E-mail: chkim@hanyang.ac.kr

Received 13 August 2015, revised 15 September 2015
Accepted for publication 28 September 2015
Published 28 October 2015

Abstract

The dose coefficients for the eye lens reported in ICRP 2010 *Publication* 116 were calculated using both a stylized model and the ICRP-110 reference phantoms, according to the type of radiation, energy, and irradiation geometry. To maintain consistency of lens dose assessment, in the present study we incorporated the ICRP-116 detailed eye model into the converted polygon-mesh (PM) version of the ICRP-110 reference phantoms. After the incorporation, the dose coefficients for the eye lens were calculated and compared with those of the ICRP-116 data. The results showed generally a good agreement between the newly calculated lens dose coefficients and the values of ICRP 2010 *Publication* 116. Significant differences were found for some irradiation cases due mainly to the use of different types of phantoms. Considering that the PM version of the ICRP-110 reference phantoms preserve the original topology of the ICRP-110 reference phantoms, it is believed that the PM version phantoms, along with the detailed eye model, provide more reliable and consistent dose coefficients for the eye lens.

Keywords: ICRP reference phantom, detailed eye model, polygon-mesh phantom, lens dose coefficients, Monte Carlo

(Some figures may appear in colour only in the online journal)

1. Introduction

The lens of the eye is very sensitive to ionizing radiation, the main health effect being induction of cataracts. The International Commission on Radiological Protection (ICRP) previously considered cataract induction as a deterministic effect with a threshold between 2 and 10 Gy and recommended annual dose limits of 150 mSv for occupationally exposed persons and 15 mSv for members of the public (ICRP 2007). However, many recent studies (Worgul *et al* 2007, Chodick *et al* 2008, Mrena *et al* 2011, Neriishi *et al* 2012) have indicated that the dose threshold for the radiation-induced cataract might be much lower than the previous values. Based on these studies, the ICRP has recommended a reduction of the occupational annual equivalent dose limit to 20 mSv, averaged over defined periods of 5 years, with no single year exceeding 50 mSv (ICRP 2012). This reduction stimulates efforts towards more accurate dosimetry for the eye lens. The ICRP-110 reference phantoms are voxel phantoms with voxel resolutions of $2.137 \times 2.137 \times 8\,\text{mm}^3$ (male) and $1.775 \times 1.775 \times 4.84\,\text{mm}^3$ (female). Due to their low resolution (ICRP 2009), the detailed eye structures cannot be represented. This limitation can be generally found in other voxel phantoms (Pujol and Gibbs 1982, Zankl *et al* 1988, Petoussi-Henss *et al* 2002, Jeong *et al* 2008, Kim *et al* 2008, Park *et al* 2014, Yeom *et al* 2014b). Therefore, for better assessment of lens dose coefficients, several investigators (Behrens *et al* 2009, Nogueira *et al* 2011, Caracappa *et al* 2014) developed detailed eye models for low-penetrative radiation, showing a steep dose gradient in the lens; eventually the ICRP adopted a detailed stylized eye model developed by Behrens *et al* (2009). The lens dose coefficients reported in ICRP *Publication* 116 (ICRP 2010) were calculated using either this detailed stylized eye model or the ICRP-110 reference phantoms, depending on radiation type, energies, and irradiation geometries. For example, for photon exposures, the detailed stylized eye model incorporated into a mathematical phantom of a head, averaged from Adam and Eva (Kramer *et al* 1982), was used to calculate lens dose coefficients up to 2 MeV for the anterior–posterior (AP), posterior–anterior (PA), lateral (LAT), and rotational (ROT) geometries, whereas above 2 MeV, the lens dose coefficients were calculated using the ICRP-110 reference phantoms. Further, the dose coefficients for the isotropic (ISO) geometry were calculated using the ICRP-110 reference phantoms for the entire energy range. Table 1 summarizes the methods used to calculate reference values of lens dose coefficients. For energies and radiation geometries not shown in table 1, as well as other radiation types (i.e. positrons, protons, muons, pions, and helium ions), the lens dose coefficients were calculated using the ICRP-110 reference phantoms. However, we believe that the use of the same computational phantom for all irradiation geometries and radiation types simplifies the dosimetric procedure.

Recently, the ICRP Committee 2 initiated a research project to convert the current voxel-type ICRP-110 reference phantoms to polygon-mesh (PM) format to address certain limitations in dose calculation due to limited voxel resolution. The ultimate goal of the conversion project is to reproduce the ICRP-110 reference phantoms in high-quality PM format, faithfully preserving the topology of their anatomical structures and, at the same time, add to them the fine structures necessary for effective dose calculations that might not be available at the original version of the phantoms. The success of the project will result in a single set of PM-version ICRP phantoms that can be used to calculate all necessary dose coefficients, for both external

Table 1. Calculation methods for lens dose coefficient used in ICRP Publication 116 (ICRP 2010).

Type of radiation	Irradiation geometry[a]	Radiation energy	Phantom used in lens dose assessment
Photon	AP, PA, LAT, and ROT	⩽2 MeV	Stylized eye model incorporated into a mathematical head phantom (average of Adam and Eva phantoms)
		>2 MeV	ICRP-110 reference phantoms
	ISO	all energies	ICRP-110 reference phantoms
Electron	AP	⩽10 MeV	Stylized eye model not incorporated into a phantom (bare eye)
		>10 MeV	ICRP-110 reference phantoms
	ISO	<1 MeV	Not calculated (adopted the dose coefficients of AP geometry)
		⩾1 MeV	ICRP-110 reference phantoms
	PA	All energies	ICRP-110 reference phantoms
Neutron	AP, LAT, and ROT	⩽4 MeV	Stylized eye model incorporated into a mathematical head phantom (UF-ORNL phantom)
		>4 MeV	ICRP-110 reference phantoms
	PA, ISO	All energies	ICRP-110 reference phantoms

[a] AP: antero-posterior; PA: postero-anterior; LAT: lateral; ROT: rotational; ISO: fully isotropic irradiation.

and internal exposure situations. An exception is the fine skeletal tissues such as endosteum and bone marrow which cannot be represented geometrically even in the PM phantoms. The use of the PM format will also enable future phantom-postural change, as necessary.

As a part of the conversion project, in the present study, we incorporated the detailed stylized eye model developed by Behrens *et al* (2009) into the phantoms that were constructed by converting the ICRP-110 reference phantom into the PM format. We believe that this approach will result in both simplification of calculation process and improved consistency in lens dose assessment. In order to determine the dosimetric effect of this incorporation, in the present study, the PM version phantoms were used to calculate lens dose coefficients for photons and electrons, and the calculated values were compared with the values specified in ICRP *Publication* 116 (ICRP 2010).

2. Material and methods

2.1. Detailed eye model

In the present study, a detailed eye model was constructed in polygon-mesh (PM) format based on the eye-model data (see figure 1, left) of Behrens *et al* (2009). Figure 1 shows both Behrens's model and its PM version.

2.2. Polygon-mesh version of ICRP-110 reference phantoms

As already mentioned, the PM versions of the ICRP-110 reference phantoms have been developed by converting the current voxel-type ICRP-110 reference phantoms (ICRP 2009) to a high-quality PM format (Yeom *et al* 2013). The PM-version phantoms maintain the topology

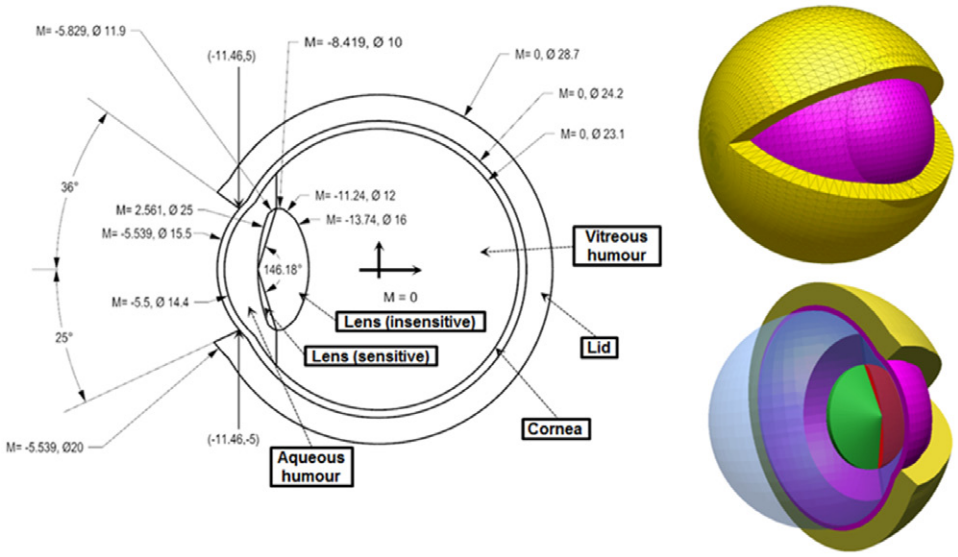

Figure 1. Detailed stylized eye model data adapted by Behrens *et al* (2009) (left) and polygon-mesh eye model constructed for the present study (right): lid (yellow), cornea (magenta), sensitive lens (red), insensitive lens (green), and humour (transparent blue).

of the ICRP-110 reference phantoms having masses matching the reference values (ICRP 2002) and, at the same time, including most of the fine structures necessary for effective dose calculation. There are some organs and tissues (i.e. bronchi, blood vessels, and muscle) that are not yet included; the corresponding spaces are temporarily filled with residual soft tissue (RST) (Lee *et al* 2007, Kim *et al* 2011, Yeom *et al* 2013). Figure 2 shows the current PM versions of the ICRP-110 reference phantoms (right) along with the voxel-type ICRP-110 reference phantoms (left).

2.3. Construction and incorporation of the detailed eye model

The detailed eye model was constructed and incorporated into the PM versions of the ICRP-110 reference phantoms following the procedure schematized in figure 3. First, from the geometrical information of the detailed eye model, a NURBS (Non-Uniform Rational B-Splines)-surface-based eye model was produced using the *Sphere, Corn* and *Boolean* functions of the *Rhinoceros* software (Robert McNeel & Associates, Seattle, Wash) which is specialized in NURBS modeling. The *Sphere* and *Corn* functions create spherical and conical NURBS-surface models, respectively. The *Boolean* function creates new NURBS model by subtracting, intersecting, or unifying two different NURBS models. The resulted NURBS eye model was then converted to PM format using the *Mesh* function which simply converts a NURBS model to a PM model, maintaining the shape. The converted PM eye model had some defects, including self-intersection and abnormal facets, which were carefully repaired by means of several refinement functions of the *Rapidform* software (INUS Technology Inc., Korea) which is specialized in PM modeling. The constructed eye model was then incorporated into the PM versions of the ICRP-110 reference phantoms using the *Transform* function of the *Rapidform* software. The *Transform* function changes a coordinate of a PM model for translation and rotation. In the course of incorporation, the centroids of the eye models were

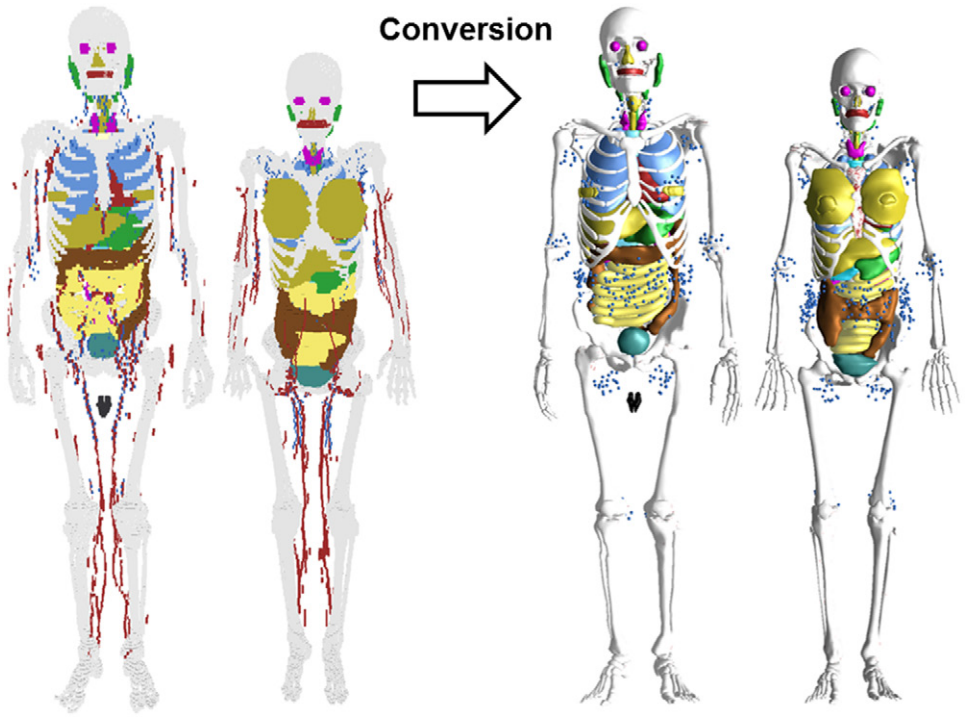

Figure 2. ICRP-110 reference phantoms (left) and their polygon-mesh (PM) versions (right).

precisely matched to the centroids of the eyes of the male phantom. For the female phantom, it was not possible to match the centroids and the positions of the eyes were thus lowered by ~3 mm in order to avoid interference of the eyes with the cranium. Thus, the centroids of the eye models in the polygon-mesh version female phantom are ~3 mm lower than the centroids of the eye models in the original ICRP-110 female phantom. Finally, the eyelids were assigned to the skin. For this, polygon facets of the skin overlapping with the eyelids were eliminated using the *Delete* function. Then, the skin and eyelids were connected using the *FillHoles* function. The connected region was carefully adjusted to produce smooth surface using the *Deform* function. For this adjustment, the total skin masses of the PM phantoms were made to match the ICRP reference values (ICRP 2002).

2.4. Dose calculations with Geant4

In order to investigate the dosimetric effect of the incorporation, the PM versions of the ICRP-110 reference phantoms along with the detailed eye model were used to calculate the dose coefficients for the eye lens. The calculated values were then compared with the ICRP *Publication* 116 data (ICRP 2010), for the following irradiation conditions: photons from 10 keV to 10 GeV in AP, PA, LAT, ROT, and ISO geometries and electrons from 100 keV to 10 GeV in AP, PA, and ISO geometries. For the Monte Carlo simulations, the code GEANT4 (version 10.01) (Agostinelli *et al* 2003) was used. In order to save computation time, we assumed that only the head of each phantom is irradiated, assuming that contribution of secondary radiations to the eye lens dose from the other part of the body is negligible

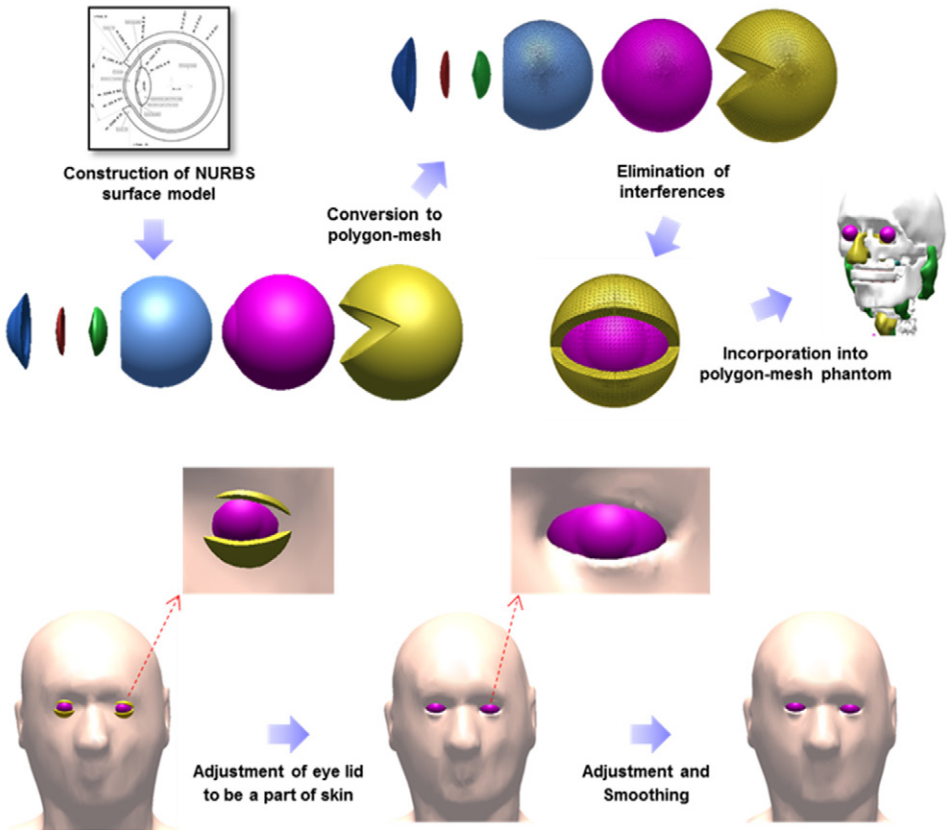

Figure 3. Incorporation procedure of detailed eye model into the PM version of the ICRP-110 reference phantoms.

(Behrens and Dietze 2011, Behrens 2013). Additionally, the PM-version phantoms were converted to the tetrahedral-mesh format using the TetGen code (Si 2015), which also significantly improves computation speed (Yeom *et al* 2014a). Finally, the phantoms were directly implemented in Geant4 (ver. 10.01), without voxelization, using the *G4Tet* solid class.

The deposited energies in the lens were calculated by *G4VPrimitiveScorer* class. The physics library of the *G4EmLivermorePhysics,* including cross section libraries of EPDL97 (Cullen *et al* 1997), EEDL (Perkins *et al* 1991), and EADL (Perkins *et al* 1997), was used with a secondary range cut value of 1 μm for photons and electrons. The number of primary particles was between 10^5–10^{10}, according to the type of particles and energies in order to keep statistical errors to less than 10%. The simulations were performed on a single core of the AMD Opteron^{TM}6176 (@ 2.3 GHz and 64GB memory).

3. Results and discussion

Figure 4 shows the PM versions of the ICRP-110 reference phantoms and the incorporated detailed eye model, and table 2 provides information on masses and densities of the different eye structures of the model as well numbers of polygons consisting the meshes. The eye model is composed of a large number (30 682) of polygon facets. The mass differences from

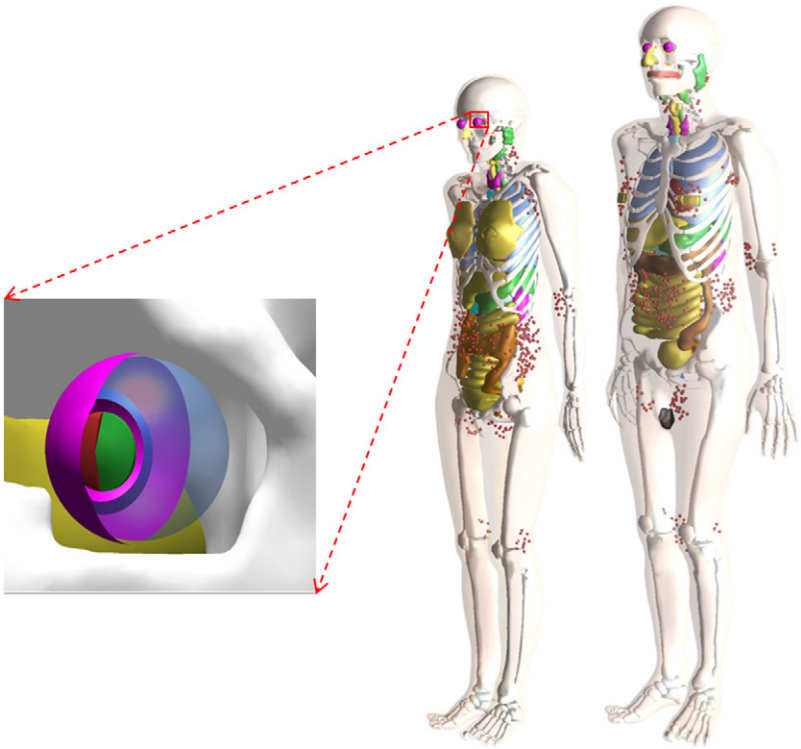

Figure 4. PM versions of ICRP-110 reference phantoms incorporating detailed eye model.

Table 2. Numbers of polygon facets, masses, and densities of the eye structures of the PM eye model constructed in the present study.

Substances	Number of polygon facets	Mass (*g*)		Mass difference (%)	Density (g cm^{-3})
		PM eye model	Original eye model		
Lens (sensitive)	1534	0.039	0.039	0.8	1.06
Lens (insensitive)	2178	0.189	0.190	0.3	1.06
Aqueous humour	2212	0.301	0.309	2.7	1.003
Vitreous humour	4838	6.014	6.045	0.5	1.0089
Cornea	4344	1.063	1.053	0.9	1.076
Lid	15576	4.682	4.864	3.7	1.09
Total	30682	12.500	12.288	1.7	—

the original stylized eye model, considering all the substances in the eye, were less than 4%; most notably, the differences for the sensitive and insensitive parts of the eye lens were negligible, i.e. 0.8% and 0.3%, respectively. Overall, the results show that the constructed eye model faithfully maintains the original structure of the detailed eye model.

Prior to comparison with the ICRP-116 data, the PM eye model constructed in the present study was validated against the stylized eye model by performing dose calculations for identical irradiation geometry. Both the polygon-mesh and the stylized model were calculated in the present study with the same simulation condition in order to investigate the effect of phantom

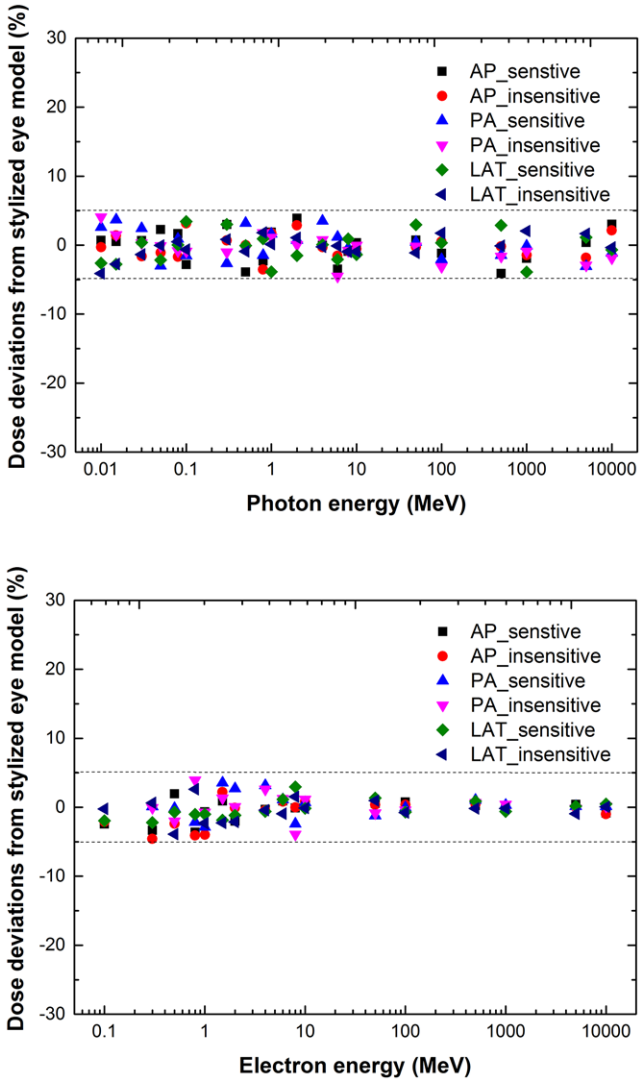

Figure 5. Dose deviation of constructed PM eye model from original stylized eye model for photon (upper) and electron (lower) exposures.

geometry (i.e. eye model type). The simulations were performed for the bare (i.e. non-phantom-incorporated) eye models using Geant4. Statistical errors of the calculated results were kept to less than 5% which is, we believe, sufficient for validation. Figure 5 shows the dose deviations of the PM version from the stylized eye model, for AP, PA and LAT irradiations and for the sensitive and insensitive regions of the lens. Note that the sensitive region is the location of stem cells associated with cataract induction (see figure 1) and the insensitive region is the entire lens region excluding the sensitive region. It can be seen that the dose deviations of the PM version from the stylized eye model were all less than 5%, thus validating the PM eye model as constructed.

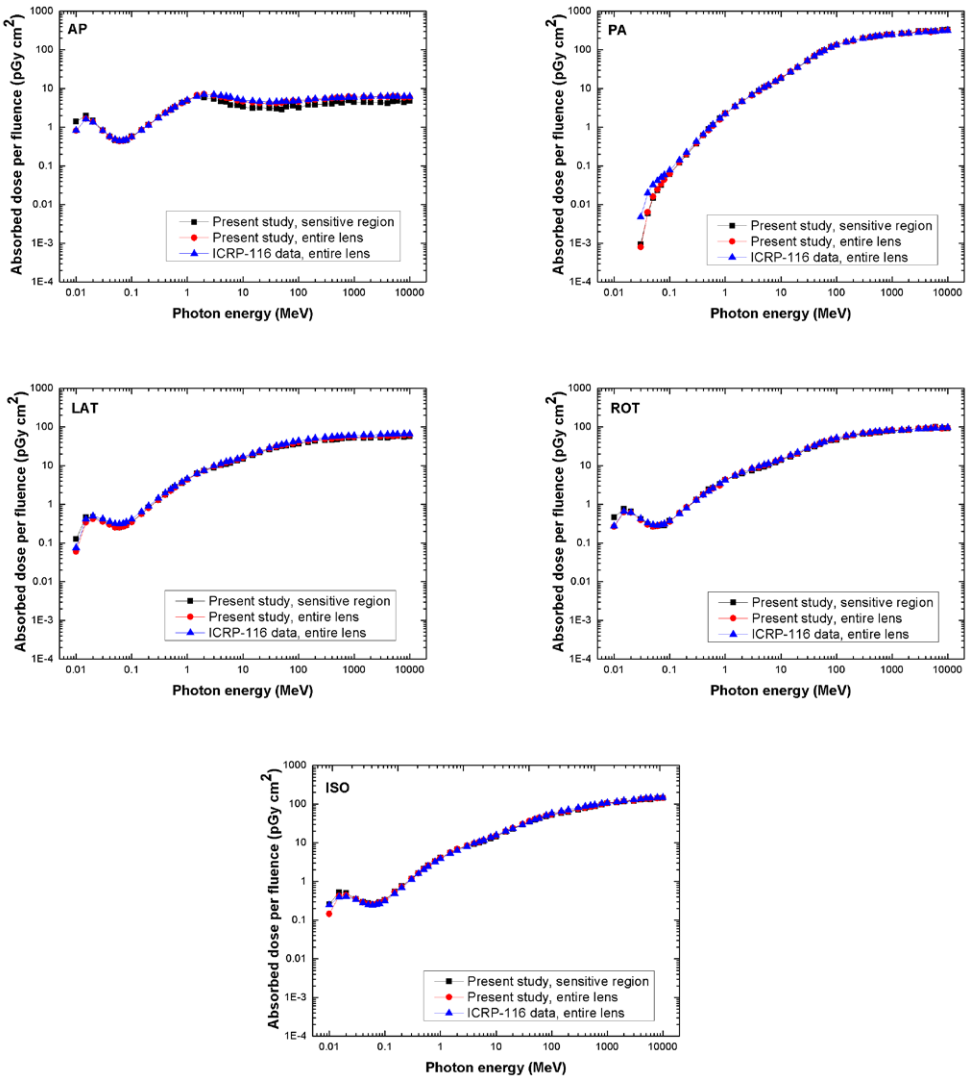

Figure 6. Dose coefficients (pGy cm^2) calculated for eye lens for photon exposures in AP, PA, LAT, ROT, and ISO geometries: PM phantom—sensitive region (black square), PM phantom—entire lens (red circle), and ICRP-116 data—entire lens (blue triangle) (ICRP 2010).

As described in section 2.4, the dose coefficients for the eye lens, defined as the absorbed dose per fluence in unit of pGy cm^2, were calculated using the PM-version phantoms with the detailed eye model; the results, were compared with the values of the ICRP-116 data (ICRP 2010). Note that the ICRP-116 *Publication* provides dose coefficients for the entire lens only, whereas the present study for the sensitive region as well.

Figure 6 compares the dose coefficients for the photon exposures in the AP, PA, LAT, ROT, and ISO irradiation geometries. In the AP geometry, the calculated dose coefficients for the entire lens showed good agreement with the ICRP-116 data; the maximum difference was 9.9% at 20 MeV. Note that AP geometry is the most important irradiation geometry for lens-dose calculation.

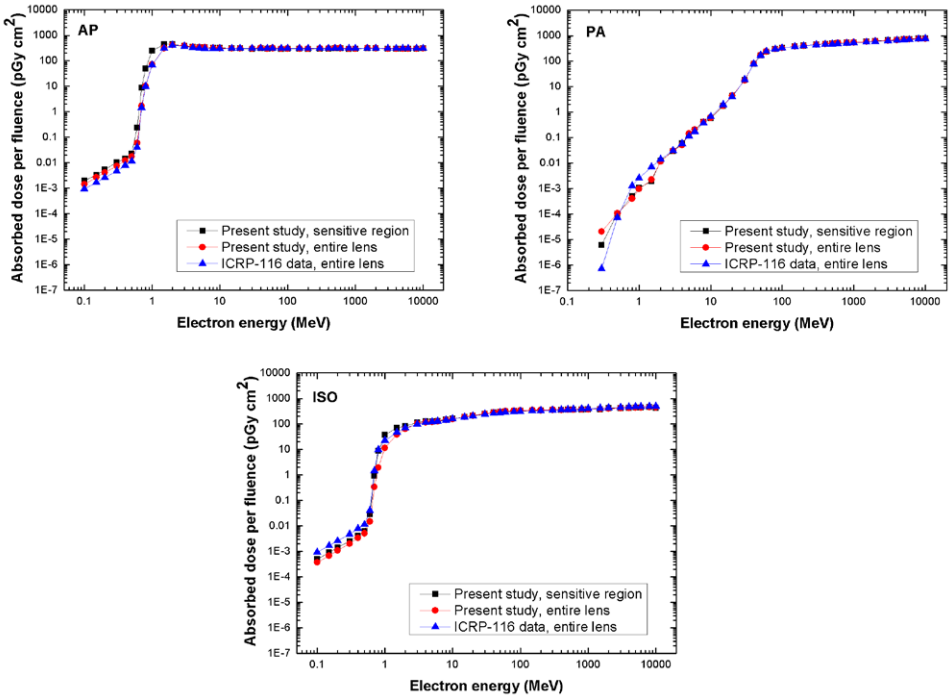

Figure 7. Dose coefficients (pGy cm^2) for eye lens for electron exposures in AP, PA, and ISO irradiation geometries: PM phantom—sensitive region (black square), PM phantom—entire lens (red circle), and ICRP-116 data—entire lens (blue triangle) (ICRP 2010).

For the PA geometry, the calculated dose coefficients showed a significant difference from the ICRP-116 data: the maximum difference was as large as ~6 times at 30 keV. This result was due mainly to the differences in head-structure size and composition between the PM versions of the ICRP-110 reference phantoms used in the present study and the mathematical phantom used to produce the ICRP-116 data (see table 1). In the LAT and ROT geometries, the differences were only moderate: the maximum differences were 21% and 11%, respectively. In the ISO geometry, there was generally good agreement: the differences were less than 9% for all energies except at 10 keV, at which the difference was 41%. This relatively large discrepancy at the low energy was due mainly to the geometrical difference between the detailed eye model and the eye models of the ICRP-110 reference phantoms used to produce the ICRP-116 data (see table 1).

From figure 6 it can be seen that, if one compares the dose coefficients of the entire and sensitive regions of the eye lens, as calculated with the PM-version phantoms, for photon energies higher than 20 keV, the dose coefficients provide similar values to, or conservative upper-bound values for, the sensitive region. However, for photon energies lower than 20 keV, the dose coefficients for the entire lens significantly underestimate those for the sensitive region. The maximum difference for the most important AP irradiation geometry was as large as ~2 times at 10 keV, which might be considered significant for some exposure situations.

Figure 7 compares the dose coefficients for AP, PA, and ISO irradiation geometries, for electron exposures. For AP geometry, the calculated dose coefficients for the entire lens showed good agreement with the ICRP-116 data for electron energies higher than 0.7 MeV:

the maximum difference was 12% at 6 MeV. For low-energy electrons (⩽0.7 MeV), however, the dose coefficients calculated with the current PM-version phantoms were much higher than the ICRP-116 data: the maximum difference was 60% at 0.2 MeV. This relatively large difference was due mainly to the fact that the ICRP-116 data were calculated using the bare-eye model for electron energies ⩽10 MeV (see table 1), and therefore do not properly reflect the dose contribution from the secondary radiations from the head structure.

For PA geometry, the difference was negligible for electron energies higher than 5 MeV, but significant for energies less than 5 MeV. At 30 keV, the maximum difference was as large as ~30 times. We believe that this was due principally to the difference of skull geometry between the PM-version phantoms (i.e. smooth surface) and the original voxel-type ICRP-110 reference phantoms (i.e. staircase-like surface). Specifically, the geometric difference near the surface of the head seems to cause significant differences in the production and/or attenuation of the secondary photons produced from the primary electrons. In addition, the difference in the codes and cross-section data also partially contribute to the dose discrepancies. This exposure situation is, however, not important for lens-dose calculation, because for PA irradiation geometry, the skin, which is directly exposed to primary electrons, is the organ of interest for dose-calculation purposes.

For the ISO geometry, the differences were negligible for electron energies ⩾2 MeV. However, for the lower electron energies, the differences were significant, the maximum difference being 81%. This divergence for electrons from 1 MeV to 2 MeV is a function of the geometrical difference between the detailed eye model used in the present study and the eye model of the ICRP-110 reference phantoms used to produce the ICRP-116 data. Note that for electron energies lower than 1 MeV, the ICRP-116 data were not calculated in the ISO geometry; instead, the values of the AP geometry were adopted as conservative estimation of the dose in the ISO geometry.

If we compare the dose coefficients for the entire and sensitive regions of the lens as calculated with the PM version phantom, we can see that those for the entire region generally provide similar values to, or conservative upper bound values for, the sensitive region of the lens. However, for some electron energies, the dose coefficients for the entire lens again significantly underestimate that for the sensitive region. The underestimation was as large as ~5.2 times at 0.7 MeV for the AP and ISO geometries, respectively.

4. Conclusion

In the present study, using anatomical information of a stylized eye model (Behrens *et al* 2009), a detailed computational model of the eye was constructed, consisting of about 30 000 polygon facets. This was then incorporated into the polygon-mesh (PM) versions of the ICRP-110 male and female reference phantoms that have been previously converted from the ICRP-110 reference voxel phantoms into PM format. The head part of the PM-version phantoms, with the detailed eye model, were then used to calculate the dose coefficients for the eye lens, and subsequently, the calculated values were compared with the values in ICRP *Publication* 116. An analysis of our results shows that generally, there exists good agreement between the calculated lens-dose coefficients in the present study and the data given in ICRP *Publication* 116. Significant differences were found for some irradiation cases, due mainly to the geometrical limitations of the phantoms used for the calculations of the eye lens dose coefficients of ICRP *Publication* 116. Considering that the PM phantoms preserve the original topology of the ICRP-110 reference phantoms, we believe that they, along with the detailed eye model, provide more reliable and consistent dose coefficients for the eye lens. This improvement can

lead to more reliable protection practices for the relevant radiation users such as interventional radiologists and cardiologists. In the present study, photons and electrons were considered and no other types of radiation. However, it is believed that their consideration would not have altered the general conclusions of this study; that is, the polygon-mesh versions of the ICRP-110 reference phantoms, along with the detailed eye models, provide more reliable and consistent dose coefficients for the eye lens.

Acknowledgments

This project was supported by Nuclear Safety and Security Commission (NSSC) through Korea Radiation Safety Foundation (KORSAFe) and also by Ministry of Science, ICT and Future Planning through the National Research Foundation of Korea (Project No.: 2011-0025496, 2012-K001146, 1403012). Two of the authors were supported by the Global PhD Fellowship program (Project No.: 2011-0007318, 2011-0030970).

References

Agostinelli S *et al* 2003 GEANT4—a simulation toolkit *Nucl. Instrum. Methods* A **506** 250–303

Behrens R, Dietze G and Zankl M 2009 Dose conversion coefficients for electron exposure of the human eye lens *Phys. Med. Biol.* **54** 4069–87

Behrens R and Dietze G 2011 Dose conversion coefficients for photon exposure of the human eye lens *Phys. Med. Biol.* **56** 415–37

Behrens R 2013 Dose conversion coefficients for electron exposure of the human eye lens: calculations including a whole body phantom *Radiat. Prot. Dosim.* **155** 224–35

Caracappa P F, Rhodes A and Fiedler D 2014 Multi-resolution voxel phantom modeling: a high-resolution eye model for computational dosimetry *Phy. Med. Biol.* **59** 5261–75

Chodick G *et al* 2008 Risk of cataract after exposure to low doses of ionizing radiation: a 20 year prospective cohort study among US radiologic technologists *Am. J. Epidemiol.* **168** 620–31

Cullen D, Hubbell J H and Kissel L 1997 *EPDL97: the Evaluated Photon Data Library, '97 Version* vol 6 (Washington, DC: Lawrence Livermore National Laboratory) UCRL-50400

ICRP 2002 Basic anatomical and physiological data for use in radiological protection: reference values *ICRP Publication 89* (Oxford: Pergamon)

ICRP 2007 The 2007 Recommendations of the international commission on radiological protection *ICRP Publication 103* (Amsterdam: Elsevier)

ICRP 2009 Adult reference computational phantoms *ICRP Publication 110* (Amsterdam: Elsevier)

ICRP 2010 Conversion coefficients for radiological protection quantities for external radiation exposures *ICRP Publication 116* (Amsterdam: Elsevier)

ICRP 2012 ICRP statement on tissue reactions and early and late effects of radiation in normal tissues and organs-threshold doses for tissues in a radiation protection context *ICRP Publication 118* (Amsterdam: Elsevier)

Jeong J H, Cho S, Cho K W and Kim C H 2008 Deformation of the reference Korean voxel male model and its effect on dose calculation *J. Radiat. Prot. Res.* **33** 167–72

Kim C H, Choi S H, Jeong J H, Lee C and Chung M S 2008 HDRK-Man: a whole-body voxel model based on high-resolution color slice images of a Korean adult male cadaver *Phys. Med. Biol.* **53** 4093–106

Kim C H, Jeong J H, Bolch W E, Cho K W and Hwang S B 2011 A polygon-surface reference Korean male phantom (PSRK-Man) and its direct implementation in Geant4 Monte Carlo simulation *Phys. Med. Biol.* **56** 3137–61

Kramer R, Zankl M, Williams G and Drexler G 1982 The calculation of dose from external photon exposures using reference human phantoms and Monte Carlo methods. Part I. The male (ADAM) and female (EVA) adult mathematical phantoms *GSF Bericht S-885* (Neuherberg: GSF)

Lee C, Lodwick D, Hasenauer D, Williams J L, Lee C and Bolch W E 2007 Hybrid computational phantoms of the male and female newborn patient: NURBS-based whole-body models *Phys. Med. Biol.* **52** 3309–33

Mrena S, Kivelä T, Kurttio P and Auvinen A 2011 Lens opacities among physicians occupationally exposed to ionizing radiation—a pilot study in Finland *Scand. J. Work Environ. Health* **37** 237–43

Neriishi K *et al* 2012 Radiation dose and cataract surgery incidence in atomic bomb survivors, 1986–2005 *Radiology* **265** 167–74

Nogueira P, Zankl M, Schlattl H and Vaz P 2011 Dose conversion coefficients for monoenergetic electrons incident on a realistic human eye model with different lens cell populations *Phys. Med. Biol.* **56** 6919–34

Park S, Yeom Y S, Kim J H, Lee H S, Han M C, Jeong J H and Kim C H 2014 Development of reference Korean organ and effective dose calculation online system *J. Radiat. Prot. Res.* **39** 30–7

Perkins S T, Cullen D E and Seltzer S M 1991 *Tables and Graphs of Electron-Interaction Cross-Sections from 10 eV to 100 GeV Derived from the LLNL Evaluated Electron Data Library (EEDL), Z = 1–100* vol 31 (Livermore, CA: Lawrence Livermore National Laboratory) UCRL-50400

Perkins S T, Cullen D E, Chen M H, Hubbell J H, Rathkopf J and Scofeld J 1997 *Tables and Graphs of Atomic Subshell and Relaxation Data Derived from the LLNL Evaluated Atomic Data Library (EADL), Z = 1–100 LLNL* (Livermore, CA: Lawrence Livermore National Laboratory) UCRL-50400-v-30

Petoussi-Henss N, Zankl M, Fill U and Regulla D 2002 The GSF family of voxel phantoms *Phys. Med. Biol.* **47** 89–106

Pujol A and Gibbs S J 1982 A Monte Carlo method for patient dosimetry from dental x-ray *Dentomaxillofac. Radiol.* **11** 25–33

Si H 2015 Tetgen, a Delaunay-based quality tetrahedral mesh generator *ACM Transactions on Mathematical Software (TOMS)* **41** 1–36

Worgul B V *et al* 2007 Cataract among Chernobyl clean-up workers: implications regarding permissible eye exposures *Radiat. Res.* **167** 233–43

Yeom Y S, Han M C, Kim C H and Jeong J H 2013 Conversion of ICRP male reference phantom to polygon-surface phantom *Phys. Med. Biol.* **58** 6985–7007

Yeom Y S, Jeong J H, Han M C and Kim C H 2014a Tetrahedral-mesh-based computational human phantom for fast Monte Carlo dose calculations *Phys. Med. Biol.* **59** 3173–85

Yeom Y S, Jeong J H, Kim C H, Ham B K, Cho K W and Hwang S B 2014b HDRK-woman: whole-body voxel model based on high-resolution color slice images of Korean adult female cadaver *Phys. Med. Biol.* **59** 3969–84

Zankl M, Veit R, Williams G, Schneider K, Fendel H, Petoussi N and Drexler G 1988 The construction of computer tomographic phantoms and their application in radiology and radiation protection *Radiat. Environ. Biophys.* **27** 153–64